CHIRALITY 16:S55–S61 (2004)

Dispersion of Anomalous Azimuthal Rotation and Circular Extinction Contrast in Dyed K_2SO_4 Crystals

WERNER KAMINSKY,* JAVIER HERREROS-CEDRÉS, MORTEN A. GEDAY, AND BART KAHR*
Department of Chemistry, University of Washington, Seattle, Washington
Dedicated to Professor Jinzo Kobayashi on the occasion of his 80th birthday and for his gift of the HAUP technique.

ABSTRACT We present measurements of the dispersion of anomalous azimuthal rotation signals from dyed crystals that are at variance with our predictions based on a model of these effects predicated on the predominance of Rayleigh scattering from isolated dye molecules (Kaminsky et al. J Phys Chem A 107:2800–2807, 2003). Here, we extend our scattering model to include the effects of the absorption and refraction of individual dyes that are inclined in a biased manner with respect to the eigenmodes of the medium. Our revised model describes the wavelength dependence of the rotations. It is likely that absorption, refraction, and Rayleigh scattering are all manifest, with absorption and refraction being the leading effects. *Chirality 16:S55–S61, 2004.*

KEY WORDS: dyed crystals; K_2SO_4; Trypan blue; azimuthal rotation; circular extinction contrast; dispersion

Many simple substances, when crystallized from solutions containing dyes, will orient and overgrow the dyes in selected growth sectors, volumes of the crystals that have advanced through a particular face in a particular direction.[1] For example, the dye trypan blue (TB) (Fig. 1) recognizes principally the chiral {111} surfaces of growing K_2SO_4 crystals by virtue of the fact that there are particular homologies between the dye conformation and the topography of the crystallographic face.[2] Dyed crystals are distinct from crystals of dyes in that oriented chromophores are dilute (~1 mole of dye per 10^4 moles of salt) and their responses to light are virtually independent from one another; their properties are uncoupled.

In a previous report, we discussed a new phenomenon in crystal optics seen in dyed crystals that is a consequence of the unusual embedding of dye transition dipoles inclined *in the same sense* with respect to the eigenmodes and mirror planes of the host.[3] This is a result of the unidirectional growth of any one growth sector. While analyzing such crystals with the High-Accuracy Universal Polarimetry (HAUP) method[4] employed in a novel scanning mode (S-HAUP), we recognized signals that mimicked intrinsic optical rotation and circular dichroism.[3] The mimicry was revealed when the sign of these effects reversed on rotating the sample or inverting the light path (flipping the sample over). Given strong oscillators remotely separated from one another, we thought that these strange effects, from here on called anomalous azimuthal rotation (AAR) and anomalous ellipticity (AE), were a likely consequence of the individual interactions of the dye molecules with the incoming light (scattering, in a general sense). We previously gave these effects the names "optical rotatory scattering" (ORS) and "circular dichroic scattering" (CDS) and attempted to explain our observations at a single wavelength on the basis of Rayleigh scattering. Our original model predicted an S-shaped wavelength dispersion for AAR and a mono-signate dispersion for AE at the absorption maximum of the dye.

Here, we present measurements of the dispersion of AAR and AE that are at variance with the early model. We extend our scattering model so as to include the effects of absorption and refraction of individual dye molecules. Our more general model describes the dispersion correctly. Absorption, refraction, and Rayleigh scattering are undoubtedly all contributing, but the latter is comparatively weak.

It has been known for decades that linear dichroism (LD) can affect the observation of optical rotation (OR) while obscuring circular dichroism (CD). Here, we not only demonstrate the obfuscation of circular effects by linear ones, but that chiroptical instruments when applied

Present address for Morten A. Geday: Clarendon Laboratory, Department of Physics, University of Oxford, Oxford OX1 3PU, UK.
Present address for Javier Herreros-Cedrés: Departamento de Física Básica, Facultad de Física, Universidad de La Laguna, La Laguna 38206, Tenerife, Spain.
Contract grant sponsors: US National Science Foundation, the Petroleum Research Fund of the American Chemical Society, FPU-research grant from the Ministerio de Educación y Cultura, Spain.
*Correspondence to: B. Kahr or W. Kaminsky, Department of Chemistry, Box 351700, University of Washington, Seattle, WA 98195-1700. E-mail: kahr@chem.washington.edu or wernerka@u.washington.edu
Received for publication 12 December 2003; Accepted 6 April 2004
DOI: 10.1002/chir.20054
Published online in Wiley InterScience (www.interscience.wiley.com).

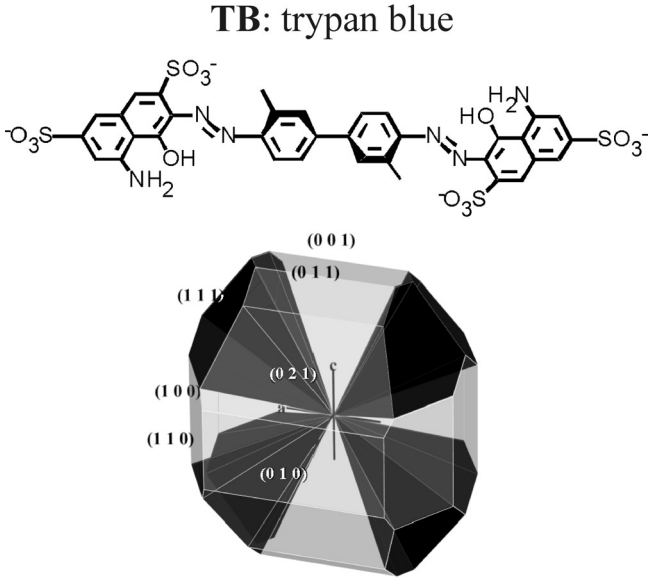

Fig. 1. Schematic of trypan blue dye that becomes oriented and overgrown within the {111} sectors of K_2SO_4 crystals.

to the specific case of a dyed sample can show signals that are easily mistaken as chiroptical signatures.

THEORY

Perturbation of the Host by the Oriented Molecular Gas

In the following we will use the Jones formalism to describe the optical phenomena observed in dyed crystals. The alternative, Mueller formalism, is equivalent for nondepolarizing systems, as in case of the dyed crystals of optical quality used in this study.[5] Table 1 summarizes relevant crystal-optical characteristics of the host, K_2SO_4. For general treatment of problems concerning the measurement of chiroptical properties in birefringent or dichroic samples, see Schellman and Jensen[6] or Schoenhoefer et al.[7]

Dye molecules absorb light anisotropically. In an isotropic medium or along the optic axis of an anisotropic crystal, the absorbance (α) along the induced dipole of the dye affects the electric field component along the dipole according to $(10^{-\alpha})^{1/2}$. The absorption perpendicular to the dipole will be addressed with an overall absorption term not explicitly shown below. The Jones matrix describing the anisotropic absorption of a dipole in its own reference system with the absorption strongest along, say, the y-axis, and zero along the x-axis of a Cartesian reference system, is then:

$$J_{Absorption}^{Dipole} = \begin{bmatrix} 1 & 0 \\ 0 & 10^{-\alpha/2} \end{bmatrix}.$$

In an anisotropic host in a birefringent direction, the absorption can only be measured along the eigenmodes e′ and e″ (Fig. 2). If the dye molecules are inclined to e″ of the host by an angle β (experimental proof of $\beta \neq 0$, see below: Fig. 8), the projections of absorbance, α' and α'', on to the eigenmodes leads to LD. The angle β is obtained from $\tan\beta = \sqrt{\frac{\alpha'}{\alpha''}}$. The Jones matrix is now recast as follows (assuming small absorbances[8] $\alpha \ll 1$, $\beta \approx 45°$, rotation matrix R for 45°, $(10^{-\alpha})^{1/2} \approx (1\text{-}\ln(10)\alpha/2) \approx (1-1.15\alpha)$)

$$J_{Absorption}^{Eigenmodes} = R^T J_{Absorption} R \approx \begin{bmatrix} 1-x & -x \\ -x & 1-x \end{bmatrix},$$

$$x = \ln(10)\alpha/4 \ll 1.$$

The effect of absorption of the dipoles can be described by projection of the light wave's field vector **E** on the direction of the induced dipole and by projection perpendicular to this direction (Fig. 3). The absorbance along the dipole is derived from α' and α'': $\alpha^{\text{dipole}} = \alpha''/\cos^2\beta$. After adding the components of the light passing the dipole, the polarization appears to be rotated by the angle $\varphi = (\beta' - \beta)$.

The angle φ changes sign upon flipping the sample 180° around one of the eigenmode directions and by 90° rotations about the wave vector of the incident light, as in the model based on Rayleigh scattering.[3] Introducing the convention that an optical rotatory effect is counted as positive when clockwise facing the light source (which means that an induced dipole inclined clockwise from the electric field vector of the incoming wave corresponds to $-\varphi$ or levorotation), we find the following Jones matrix describing AAR as a result of the absorbance of the dye measured along the eigenmodes of the host crystal:

$$J_{AAR} \approx \begin{bmatrix} 1 & \varphi \\ \varphi & 1 \end{bmatrix}, \varphi = \frac{-1.15\alpha''}{1-1.15\alpha''}; \alpha'' \ll 1; \beta = 45°$$

(φ in rad). This matrix is of the same form of that used in our ORS model.[3] We thus can use our previous mathe-

TABLE 1. Basic crystallographic and optical data for the host crystal K_2SO_4

optical character	2^+
refractive indices[8]	$n_a = 1.4928$, $n_b = 1.4916$, $n_c = 1.4954$
point group	mmm (D_{2h})
lattice parameters (Å)[9]	a = 5.773, b = 10.023, c = 7.484

Corresponding values from dyed sectors remained within the standard deviation of the pure salt. Standard deviations are ±1 of the last given digits.

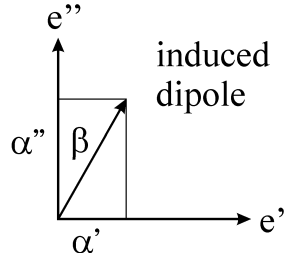

Fig. 2. Projection of the absorbance of a dipole on the eigenmodes of a crystal.

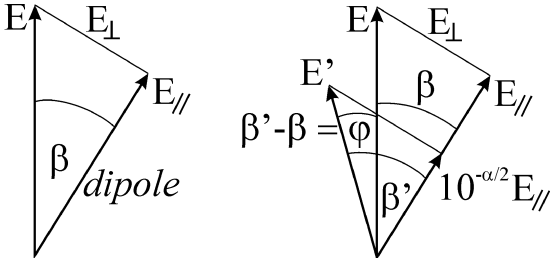

Fig. 3. Model for azimuthal rotation based on absorption of dipoles inclined towards the eigenmodes of the host. It is assumed that the perturbation to the refractivity of the host crystal due to the dye molecules is small.

matical description to set up the Jones matrix combining AAR and linear birefringence (LB) (See Appendix A for a summary of the derivation of the Jones matrix $J_{AAR,\,LB}$ for a birefringent crystal exhibiting AAR). The addition of birefringence requires the simultaneous treatment of absorption and refraction[3] giving the following Jones matrix for the linearly birefringent sample with inclined oscillators in resonance:

$$J_{AAR,\,LB} = \begin{bmatrix} e^{i\varkappa} & \frac{\varphi}{\varkappa}\sin\varkappa \\ \frac{\varphi}{\varkappa}\sin\varkappa & e^{-i\varkappa} \end{bmatrix}, \quad \varkappa = \delta/2, \delta = \frac{2\pi L \Delta n}{\lambda}.$$

Here, δ is the phase factor, φ is the azimuth of linearly polarized light due to the inclined dipoles as defined in J_{AAR}, Δn is the double refraction of the sample, and λ the wavelength of the incident light.

In HAUP measurements azimuthal rotations are unfolded from the direction of the eigenmodes of a birefringent crystal. In the absence of birefringence a circular dichroic sample causes linearly polarized light to become elliptically polarized. However, if the sample is birefringent and exhibits circular dichroism, this would affect the HAUP reading of the eigenmode directions. In our S-HAUP experiments, we indeed observed anomalous ellipticity (AE), manifest as a change of the apparent eigenmode direction. However, this signal showed a strong dispersion. AE seemed to vanish where the absorption of the dye is strongest. The easiest way to understand AE is to assume that the dipoles create a birefringent subsystem, described by the Jones matrix:

$$J_{AE} = R^T \begin{bmatrix} e^{i\varkappa} & 0 \\ 0 & e^{-i\varkappa} \end{bmatrix} R \approx \begin{bmatrix} 1 & i\varkappa \\ i\varkappa & 1 \end{bmatrix}, \quad \varkappa = -\Delta/2 \ll 1,$$

where exp(-ix) ≈ 1-ix, Δ is the phase factor of the birefringent subsystem, and R is a matrix rotation by angle β, close to 45° for TB in the (111) sectors of K_2SO_4. The dispersion of Δ_{dipoles} for this model would be that of refraction or S-shaped, i.e., the Kramers-Kronig transform of the absorption to which the azimuthal rotation is correlated. However, quantitative analysis using the Kramers-Kronig relation requires precisely determined line shapes of the absorption bands, obscured here because of broad overlapping transitions.

Observations With a Circular Extinction Contrast Imaging Microscope

Our interest in dyed K_2SO_4, which led to the surprising observation of AAR and AE, stemmed from our desire to detect chiroptical signatures of dye molecules enantioselectively embedded in the crystal and to correlate enantiomeric conformation to the chirality of the (111) sectors with which they were associated. The previously described S-HAUP experiments[3] were originally motivated to measure the intrinsic optical rotation. In order to detect circular extinction in a great variety of materials, we recently invented a circular extinction (CE) contrast imaging microscope (CEIM).[9] This measures the differential transmission of left and right circularly polarized light. We will soon reveal that it did not show the expected effect, intrinsic AE or CD, but contrast that is related to AAR when trained on some dyed crystals.[10] When detected with the CEIM, the AAR effect might be better described phenomenologically as anomalous circular extinction (ACE). However, we will use the AAR acronym throughout so as not to propagate jargon.

The optical train in a standard CE contrast measurement in the Jones formalism begins with the following amplitudes of circularly polarized waves:

$$A_\pm = \frac{1}{\sqrt{2}} \begin{bmatrix} 1 \\ \pm i \end{bmatrix} \mathrm{E}_0.$$

In the dyed K_2SO_4 sample that we now know to possess LB and AAR, the amplitudes $A'_\pm$ are then:

$$A'_\pm = \begin{bmatrix} A'_{1\pm} \\ A'_{2\pm} \end{bmatrix} = J_{AAR,LB} = \begin{pmatrix} e^{i\varkappa} & \frac{\varphi}{\varkappa}\sin\varkappa \\ \frac{\varphi}{\varkappa}\sin\varkappa & e^{-i\varkappa} \end{pmatrix} \frac{1}{\sqrt{2}} \begin{bmatrix} 1 \\ \pm i \end{bmatrix} E^0$$

$$= \begin{pmatrix} e^{i\varkappa} \pm i\frac{\varphi}{\varkappa}\sin\varkappa \\ \frac{\varphi}{\varkappa}\sin\varkappa \pm i e^{-i\varkappa} \end{pmatrix} \frac{1}{\sqrt{2}} E^0$$

$$= \begin{pmatrix} \cos\varkappa + i\sin\varkappa \pm i\,\frac{\varphi}{\varkappa}\sin\varkappa \\ \frac{\varphi}{\varkappa}\sin\varkappa \pm i\cos(-\varkappa)\mu\sin(-\varkappa) \end{pmatrix} \frac{1}{\sqrt{2}} E_0$$

The intensities follow from:

$$A'^{*}_\pm \cdot A'_\pm = \frac{1}{2} E_0^2 (A'^{*}_{1\pm} A'_{1\pm} + A'^{*}_{2\pm} A'_{2\pm})$$

$$= E_0^2 \{\cos^2\varkappa + (\sin\varkappa \pm \frac{\varphi}{\varkappa}\sin\varkappa)^2\}$$

and we find indeed a difference in light intensities for the transmission of left and right circularly polarized light:

$$\frac{I'_\pm}{E_0^2} = 1 \pm 2\varphi\frac{\sin^2\varkappa}{\varkappa} + \varphi^2\frac{\sin^2\varkappa}{\varkappa^2}.$$

Thus, differential circular extinction contrast:

$$\frac{I'_+ - I'_-}{I_0} = 4\varphi\frac{\sin^2\delta/2}{\delta/2}$$

can result, but only if the sample is birefringent and the phase $\delta \neq n2\pi$, where n = 1, 2, 3....

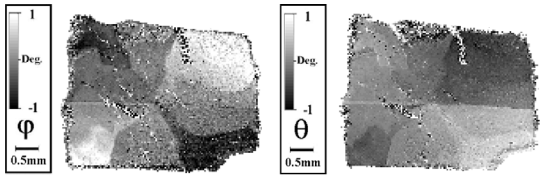

Fig. 4. Anomalous azimuthal rotation (φ) and anomalous eigenray direction ($\theta=\theta_0-\eta/\delta$) in dyed K_2SO_4 measured with the S-HAUP system at 635nm. θ, the apparent eigenray direction, is a function of the intrinsic eigenray direction (θ_0) and the anomalous ellipticity effect (η) scaled by the phase shift (δ). Angles φ and θ are counted clockwise looking towards the light source.

Paradoxically, AE is not manifest as circular extinction contrast, regardless of the value of δ. The corresponding analysis using J_{AE} leads to zero intensity difference between transmitted left and right circularly polarized light.

EXPERIMENTAL

In addition to images of anomalous azimuthal rotation (AAR) and ellipticity (AE) at 670 nm, the S-HAUP system was equipped with two additional lasers operating at 532 nm and 635 nm. The S-HAUP device, its specifications and some applications have been described previously.[11] The main difference with respect to standard HAUP instruments is that we rotate the polarizer and analyzer and leave the sample orientation constant to enable sample scanning. We studied the theory of HAUP to determine whether the difference of AAR and AE to intrinsic OR and CD would affect the measurements and concluded that the first notable differences occur in negligibly small high-order contributions to the biquadratic polynomial describing the intensity of light as a function of polarizer and analyzer modulations (Appendix B).[3]

The observed effects are far larger than parasitic ellipticities of the instrument. The device reliably detects optical rotations as small as 5×10^{-3} degrees. Our observations are in the range of 1°. Instead of producing images of the so-called HAUP quantity $B_0 = (\gamma-2\varphi/\delta)\sin(\delta)$ and A_0, a function depending on the eigenray directions, which in our case is different from standard HAUP, we adjusted the thickness of the sample to ensure a nonzero value of $\sin(\delta)$ and plotted the azimuthal rotation φ and apparent eigenray

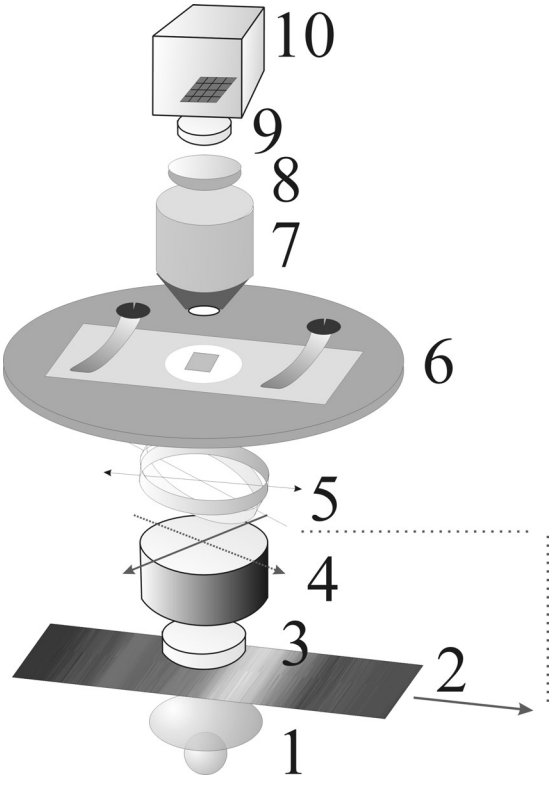

Fig. 5. Visible light circular extinction imaging microscope (CEIM). Schematic omits motors and mounts. (1) light source (2) variable interference filter (3) depolarizer (4) rotating polarizer (5) tilting λ/4-compensator (6) sample mount (7) objective (8) projector lens (9) depolarizer (10) CCD-camera.

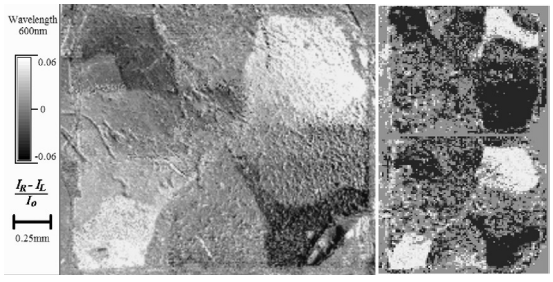

Fig. 6. Anomalous circular extinction contrast images of dyed K_2SO_4 measured at a wavelength of 600 nm. The false color-coded CE signal shows alternative signs in neighboring sectors. The smaller pictures on the right show that the CE in each of the colored sectors changes sign when the sample is flipped about a horizontal axis. The antisymmetry of the sign of the signal with respect to the wavevector is inconsistent with intrinsic CD.

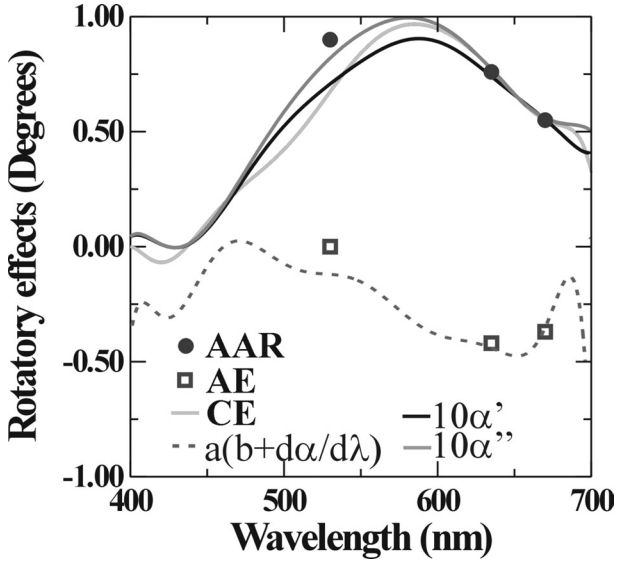

Fig. 7. Dispersion of anomalous rotatory properties. The discrete measurements were obtained with selected lasers in the S-HAUP system. The AAR signal was derived from $(I_+-I_-)/I_0$ with the CE - microscope, scaled by the factor $(180/4\pi)\{(\delta/2)/[\sin^2(\delta/2)]\}$ in 80μm (010) section of K_2SO_4/TB crystal ($\Delta n = 0.00260$).[2] This factor has a value of ca. 20° *a* and *b* are scaling factors.

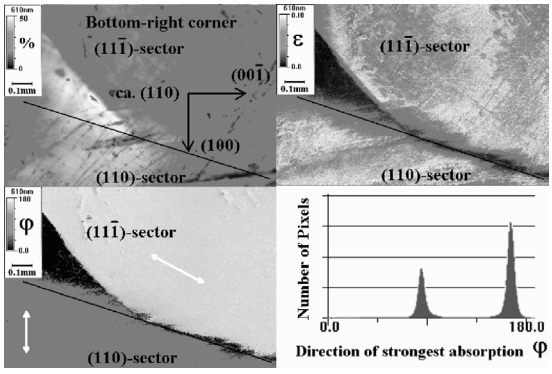

Fig. 8. K_2SO_4 crystal dyed with trypan blue cut perpendicular to the optic axis that is approximately the [110] direction. The diagonal black line roughly divides regions of the section that traverse the heavily dyed (111) sector and the lighly dyed (110) sector. Upper left: live camera image. Upper right: magnitude of the linear dichroism (ε, defined in the text). Lower left: orientation of the strongly absorbing direction measured counterclockwise from the horizontal axis. Arrows in upper right and lower left indicate the directions of the transition dipole moments. Lower right: histogram of the strongest absorbing direction. It is bi-valued indicating distinct behaviors in the two growth sectors.

direction Θ directly. The phase δ varies insignificantly over the plane parallel cut and polished sample plates.

As an example of the manifestation of AAR and AE in dyed crystals, we show corresponding images at 635 nm that compare well with those at 670 nm reported previously[3] (Fig. 4). The angle Θ in the HAUP scans consists of two contributions, i.e., eigenray directions of the birefringent host crystal plus η/δ, the ellipticity signal (in ellipsometric units) normalized to the phase δ.

A more comprehensive treatment of the dispersion was achieved with the CEIM.[5,12] The new microscope can reach a higher spatial resolution than the S-HAUP system and produces continuous spectra of absorbance and CE contrast that are impractical with a laser-based polarimeter (Fig. 5). To obtain CE contrast measurements on birefringent samples, a linear polarizer is alternately driven to +45° and −45° with respect to the extinction directions of a $\lambda/4$ retarder that is tuned by tilting about an eigenmode perpendicular to the light path to compensate for dispersion. Tilting the retarder changes the path length and the elliptic cross-section traversed by the incident light and thereby the effective birefringence of the retarder. This ensures the integrity of alternating right and left circularly polarized light produced at all wavelengths selected by a variable interference filter.

The difference of the two images, normalized by the regular absorption of the sample, yields the uncorrected CE contrast per pixel in terms of $(I_{45°}-I_{-45°})/I_o$. After storing the integrated data, the interference filter is advanced to another wavelength and the $\lambda/4$-compensator is adjusted accordingly. The device can obtain CE spectra of a heterogeneous sample from a region as small as a few pixels of a 640 × 480-pixel image. Details of the device have been published elsewhere.[11]

We obtained images with the CEIM similar to those from the S-HAUP system. They were invariant to sample rotation, as expected when measuring with near perfect circularly polarized light, but showed a change of sign upon flipping the sample over (Fig. 6). This indicates that the observation is not intrinsic CD, but AAR.

With the CE microscope we were able to produce AAR spectra between 400 and 700 nm. Figure 7 shows the results, with the AAR signal from the red sector on the top right in Figure 6, measured as $(I_+-I_-)/I_0$, and scaled by $(180/4\pi)\{(\delta/2)/[\sin^2(\delta/2)]\}$. Added to Figure 7 are the absorbances in orthogonal polarizations α' and α'', scaled by a factor 10, and the derivative of absorption scaled to fit the AE data. The derivative is only a rough approximation of the Kramers-Kronig transform but is nevertheless illustrative. Because TB has at least two absorption bands, a quantitative treatment of AAR and AE has not been attempted.

Measurements in other crystals differing in dye content normalized to the dye concentration agreed with the present results.

DISCUSSION

The dispersion of AAR closely follows the absorbance of the dye molecules, leading us to believe that absorption as discussed in the Theory section is the leading term in AAR. Our model based solely on Rayleigh scattering predicts an S-shaped dispersion. Such scattering certainly occurs, but seems to play only a minor role in the AAR signal. An S-shaped dispersion is observed in the AE measurement (at least as far we can tell from measurements at only three wavelengths). Again, this behavior is the opposite of that predicted from Rayleigh scattering.

We observe good agreement between AAR measurements from the S-HAUP device and those from the CE-microscope. However, when we try to compare the absorbance with the AAR signal, we find a significant mismatch: from the maximum absorbance of ~0.1 we would expect an AAR signal as large as $0.1*1.15*(180/\pi)/(1-0.1*1.15)$. = 7.5°, much larger than that observed experimentally. It could be that a crucial assumption in our model, that *all* dye molecules are aligned at the same angle toward the eigenmodes of the host, is not valid. To be consistent with our model, only ~13% of molecules can be aligned; the remainder of the absorbance comes from an effectively random distribution.

The selected absorption of inclined dipoles leads to a rotation that should predict whether the dipoles are inclined at 45° or −45° with respect to the linear polarization in the S-HAUP experiment. The model predicts that the dyes are inclined so that they are roughly *perpendicular* to the growth faces, not parallel, as predicted by the scattering model and represented in Figure 10 in Ref. 3.

In order to confirm that the new prediction was correct, we cut a crystal of K_2SO_4 containing TB perpendicular to the optic axis that is approximately the (110) direction. This cut is shown in Figure 8. The diagonal black lines divide regions in the section that traverse the heavily dyed (111) sector and the lightly dyed (110) sector. The LD in this section was quantified by using the rotating polarizer method.[13] This technique produces separate maps of the magnitude of the LD (ϵ) and the orientation of the

transition dipole moment (φ). The LD is measured in terms of the scaled differential transmission Δk along the eigenmodes of the sample, where $\epsilon = 2\pi L\Delta k/\lambda$ and $\Delta k = 2(T_{0^\circ} - T_{90^\circ})/(T_{0^\circ} + T_{90^\circ})$. $T_{0^\circ,90^\circ}$ are the transmissions along the primary polarization directions. The LD is just a small fraction of the theoretical maximum—it does not exceed 0.15—in complete agreement with the measured rotations in the S-HAUP experiments. Moreover, the orientation is as predicted by the model described herein.

ACKNOWLEDGMENTS

We are most grateful for the support of this work through grants from the US National Science Foundation, the Petroleum Research Fund of the American Chemical Society and the FPU-research grant from the Ministerio de Educación y Cultura (Spain).

APPENDIX A

Optical properties are often productively comprehended by viewing bulk effects as the consequence of operators for N infinitesimal layers. In our case, φ represents AAR after passing through the whole crystal and δ is the phase factor in the Jones matrix for LB, J_{LB}, given below. The properties of the thin layer are estimated up to the order of N^{-2} from the product of J_{AAR} and J_{LB}:

$$J_{LB} = \begin{bmatrix} e^{i^\delta/2} & 0 \\ 0 & e^{-i^\delta/2} \end{bmatrix} J_{AAR} \approx \begin{bmatrix} 1 & \varphi \\ \varphi & 1 \end{bmatrix}$$

$$J_{layer} = J_{AAR}J_{LB} \approx \begin{bmatrix} 1 + i\delta/2N & \varphi/N \\ \varphi/N & 1 - i\delta/2N \end{bmatrix}$$

$$= \left(1, -i\frac{\delta}{2N}, -i\frac{i\varphi}{N}\right)\left(\begin{bmatrix} 1 & 0 \\ 0 & 1 \end{bmatrix}, \begin{bmatrix} -1 & 0 \\ 0 & 1 \end{bmatrix}, \begin{bmatrix} 0 & 1 \\ 1 & 0 \end{bmatrix}\right)$$

$$= \left(1, -\frac{i}{N}T_1, -\frac{i}{N}T_2\right)\left(\sigma_0, \sigma_1, \sigma_2\right)$$

$$= \sigma_0 - \frac{i}{N}T \cdot \sigma$$

According to Schellman and Jensen,[6] product matrix can be expressed in terms of the Pauli spin matrices or spinors, σ_0, σ_1, and σ_2. The Jones matrix of the whole crystal follows from:

$$J_{crystal} = (\sigma_0 - \frac{i}{N}\mathbf{T} \cdot \sigma)^N \approx e^{-iT\cdot\sigma}$$

Where $\mathbf{T}$ is a mixed circular and linear phase.

With $\mathrm{n} = \frac{\mathrm{T}}{|\mathrm{T}|}$; $|\mathrm{T}| \underset{\varphi \ll \delta}{\longrightarrow} \frac{\delta}{2}$; $(\mathrm{n}\cdot\boldsymbol{\sigma})^{2j} = \boldsymbol{\sigma}_0, j = 1,2,3,\ldots$ follows:

$$J_{crystal} = e^{-i\frac{\delta}{2}\mathbf{n}\cdot\boldsymbol{\sigma}} = \sigma_0 - i\frac{\delta}{2}\mathbf{n}\cdot\sigma$$

$$-\frac{1}{2!}\left(\frac{\delta}{2}\mathbf{n}\cdot\sigma\right)^2 + \frac{i}{3!}\left(\frac{\delta}{2}\mathbf{n}\cdot\sigma\right)^3 + -\ldots$$

$$= \sigma_0\left[1 - \frac{1}{2!}\left(\frac{\delta}{2}\right)^2 + \frac{1}{4!}\left(\frac{\delta}{2}\right)^4 - + \ldots\right]$$

$$-i\mathbf{n}\cdot\sigma\left[\frac{\delta}{2} - \frac{1}{3!}\left(\frac{\delta}{2}\right)^3 + -\ldots\right]$$

$$= \sigma_0\cos\frac{\delta}{2} - i\mathrm{n}\cdot\sigma\sin\frac{\delta}{2} = \begin{bmatrix} e^{i\frac{\delta}{2}} & \frac{2\varphi}{\delta}\sin\frac{\delta}{2} \\ \frac{2\varphi}{\delta}\sin\frac{\delta}{2} & e^{-i\frac{\delta}{2}} \end{bmatrix}$$

If φ is replaced by an in-phase component, $i\eta$; the above treatment produces the Jones matrix for an anomalously elliptic (AE) and linearly birefringent crystal. The difference in the Jones matrices describing AAR and AE is that the off-diagonal terms have the same sign, whereas in case of OR and CD, the signs would be different.

APPENDIX B

In a HAUP-related experiment, the sample at extinction angle Θ_0 is placed between two orthogonal polarizers that are rotated about small angles Y and Ω. The optical train in this case is represented by a string of matrices where A is the light amplitude with rotation matrices for the polarizer (R_Y), analyzer (R_Ω), and sample ($R_{\Theta 0}$), and parasitic ellipticities of polarizer and analyzer $(\bar{R}_p), (\bar{R}_q)$:

$$A = \bar{R}_q^t R_\Omega^t \begin{bmatrix} 0 & 0 \\ 0 & 1 \end{bmatrix} R_\Omega \bar{R}_q R_\theta^t J R_\theta R_Y \bar{R}_p \begin{bmatrix} 1 \\ 0 \end{bmatrix},$$

with:

$$R_\Omega = \begin{bmatrix} \cos\Omega & -\sin\Omega \\ \sin\Omega & \cos\Omega \end{bmatrix}, R_Y = \begin{bmatrix} \cos Y & -\sin Y \\ \sin Y & \cos Y \end{bmatrix},$$

$$R_\theta = \begin{bmatrix} \cos\theta_0 & -\sin\theta_0 \\ \sin\theta_0 & \cos\theta_0 \end{bmatrix}, \bar{R}_q = \begin{bmatrix} 1 & -iq \\ iq & 1 \end{bmatrix},$$

$$\bar{R}_p = \begin{bmatrix} 1 & -ip \\ ip & 1 \end{bmatrix}$$

and

$$J = \begin{bmatrix} e^{i\frac{\delta}{2}} & \frac{2(\varphi+i\eta)}{\delta}\sin\frac{\delta}{2} \\ \frac{2(\varphi+i\eta)}{\delta}\sin\frac{\delta}{2} & e^{-i\frac{\delta}{2}} \end{bmatrix},$$

representing AAR (φ) and AE (η).

For a treatment including parasitic ellipticities and the Δy-error (misalignment of polarizer and analyzer), see also Ref. 13.

The result of these operations is written approximately as a biquadratic polynomial that is normalized to the amplitudes of Y^2 and Ω^2:

$$I/I_0 = A \cdot A^\Omega = a_0 + a_1\Omega + a_2 Y + a_3\Omega Y + a_4\Omega^2 + a_5 Y^2 + a_6\Omega^2 Y + a_7\Omega Y^2 + a_8\Omega^3 + a_9 Y^3$$

with:

$$\begin{aligned} a_1 &= 2\left[\left(\frac{\varphi}{\delta} + p\right)\sin\delta + \left(\frac{\eta}{\delta} - \theta\right)(1 - \cos\delta)\right], \\ a_2 &= 2\left[\left(\frac{\varphi}{\delta} - q\right)\sin\delta + \left(\frac{\eta}{\delta} - \theta\right)(\cos\delta - 1)\right], \\ a_3 &= 2\cos\delta, a_4 = a_5 = 1, \end{aligned}$$

$$a_6 = \left(\frac{\eta}{\delta} - \theta\right)(1 - \cos\delta),$$

$$a_7 = 4\left(\frac{\eta}{\delta} - \theta\right)(\cos\delta - 1),$$

$$a_8 = -\frac{4}{3}\left[\left(\frac{\varphi}{\delta} + p\right)\sin\delta + \left(\frac{\eta}{\delta} - \theta\right)(1 - \cos\delta)\right],$$

$$a_9 = -\frac{4}{3}\left[\left(\frac{\varphi}{\delta} - q\right)\sin\delta + \left(\frac{\eta}{\delta} - \theta\right)(\cos\delta - 1)\right]$$

(Compare this with the case of intrinsic CD and OR: If the component J_{12} is negative in the Jones matrix describing chiroptical properties in the presence of birefringence, then differences to above occur in

$$a_6 = -4\left[\frac{\varphi}{\delta}\sin\delta + \theta(1 - \cos\delta)\right],$$

$$a_7 = -4\left[\frac{\varphi}{\delta}\sin\delta + \theta(\cos\delta - 1)\right]).$$

When allowing for a misalignment of the kind $\Omega = \Omega' + (\delta Y)$, the polynomial transforms according to:

$$I/I_0 = b_0 + b_1\Omega' + b_2 Y + b_3\Omega' Y + b_4\Omega'^2 + b_5 Y^2 + b_6\Omega'^2 Y + b_7\Omega' Y^2 + b_8\Omega'^3 + b_9 Y^3$$

where the b_i coefficients are given by:

$$b_1 = a_1 + 2(\delta Y)\,a_4, b_2 = a_2 + (\delta Y)a_3, b_3 = a_3 + 2(\delta Y)a_6,$$

$$b_4 = a_4 + 3(\delta Y)a_8, b_5 = a_5 + (\delta Y)a_7,$$

$$b_6 = a_6,\ b_7 = a_7,\ b_8 = a_8,\ b_9 = a_9.$$

The first term (b_0) is the overall offset in the intensity measurement. Parameters φ and Θ are found from combinations of the parameters ai}:

$$[\varphi/\delta + (p - q)]\sin\delta + \frac{1}{2}\delta Y(1 + \cos\delta) = \frac{1}{4}(a_1 + a_2)^{16} \sim \varphi\sin\delta/\delta$$

$$\theta(\theta_0, \eta)(1 - \cos\delta) + [p + q]sin\delta + \frac{1}{2}\delta Y(1 - \cos\delta) = \frac{1}{4}(a_2 - a_1) \sim \theta(\theta_0, \eta)(1 - \cos\delta),$$

if parasitic effects are small compared to φ and Θ.

The first differences between intrinsic OR and CD and AAR and AE, respectively, appear in terms of order $Y\Omega^2$ and ΩY^2, which are negligibly small for typical modulation amplitudes that do not exceed 1°. Otherwise, these equations are of exactly the same form as previously reported for intrinsic OR and CD.

LITERATURE CITED

1. Kahr B, Gurney RW. Dyeing crystals. Chem Rev 2001;101:893–951.
2. Bastin L, Kahr B. Engineering oriented gases: dyeing K_2SO_4. Tetrahedron 2000;56:8250–8260.
3. Kaminsky W, Geday MA, Herreros-Cedrés J, Kahr B. Optical rotatory and circular dichroic scattering. J Phys Chem A 2003;107:2800–2807.
4. Kobayashi J, Uesu Y. A new optical method and apparatus 'HAUP' for measuring simultaneously optical activity and birefringence of crystals. I. Principles and construction. J Appl Cryst 1983;16:204–211.
5. Azzam RMA, Bashara NM. Ellipsometry and polarized light. Amsterdam: North-Holland; 1977.
6. Schellman J, Jensen HP. Optical spectroscopy of oriented molecules. Chem Rev 1987;87:1359–1399.
7. Schoenhoefer A, Kuball H-G, Puebla C. Optical activity of oriented molecules. IX. Phenomenological Mueller matrix description of thick samples and of optical elements. Chem Phys 1983;76:453–467.
8. If the angle β differs from 45°, we can split the Jones matrices in two with one describing LD oriented along the eigen modes and one for LD inclined at 45° to the eigen mode directions.
9. Claborn K, Puklin-Faucher E, Kurimoto M, Kaminsky W, Kahr B. Circular dichroism imaging microscopy: application to enantiomorphous twinning in biaxial crystals of 1,8-dihydroxyanthraquinone. J Am Chem Soc 2003;103:14825–14831.
10. Intrinsic CD of dyed polycrystalline amyloid was observed with the CEIM (to be published).
11. Kaminsky W, Glazer AM. Measurement of optical rotation in crystals. Ferroelectrics 1996;183:133–141. Kaminsky W. Reinvestigation of optical activity in the course of the ferroeleastic phase transition in cadmium langbeinite, $K_2Cd_2(SO_4)_3$. Phase Transitions 1996;59:121–133. Kaminsky W. Topographies of chiral and associated optical properties in $FeBO_3$ using a novel polarimeter, the 'tilter.' Ferroelectrics 1997;204:233–246. Mucha D, Stadnicka K, Kaminsky W, Glazer AM. Determination of optical activity in monoclinic crystals of tartaric acis, (2R, 3R)-(+)-$C_4H_6O_6$, using the tilter. J Phys Condens Matter 1997;9:10829–10842. Kim D-Y, Kaminsky W, Glazer AM. A low-temperature tilter system and its application to measurement of the anisotropy of optical rotation in K_2ZnCl_4 in the vicinity of the phase transition at 145K. Phase Transitions 2001;73:533–563. Kaminsky W, Thomas PA, Glazer AM. Optical rotation in $RbTiOAsO_4$ (point group mm2). Z Kristallogr 2002;217:1–7.
12. Claborn K, Jang S-H, Su F, Kaminsky W, Kahr B. Circular extinction imaging of twin laws in dye-doped crystals. J Phys Chem (submitted).
13. Glazer AM, Lewis JG, Kaminsky W. An automatic optical imaging system for birefringent media. Proc R Soc Lond A 1996;425:2751–2765.
14. This term corresponds to the B-term in standard HAUP experiments, see Ref. 4.